Neurobiology of Disease 106 (2017) 133–146

Contents lists available at ScienceDirect

Neurobiology of Disease

journal homepage: www.elsevier.com/locate/ynbdi

Sirtuin 3 rescues neurons through the stabilisation of mitochondrial biogenetics in the virally-expressing mutant α-synuclein rat model of parkinsonism

Jacqueline A. Gleave [a,1], Lindsay R. Arathoon [a,1], Dennison Trinh [a,1], Kristin E. Lizal [a], Nicolas Giguère [b,c], James H.M. Barber [a], Zainab Najarali [a], M. Hassan Khan [a], Sherri L. Thiele [a], Mahin S. Semmen [a], James B. Koprich [d], Jonathan M. Brotchie [d], James H. Eubanks [d], Louis-Eric Trudeau [b,c], Joanne E. Nash [a,*]

[a] Centre for the Neurobiology of Stress, Department of Biological Sciences, University of Toronto Scarborough, Toronto, Ontario, Canada
[b] Department of Pharmacology, Central Nervous System Research Group (GRSNC), Faculty of Medicine, Universite de Montreal, Montreal, Quebec, Canada
[c] Department Neuroscience, Central Nervous System Research Group (GRSNC), Faculty of Medicine, Universite de Montreal, Montreal, Quebec, Canada
[d] Krembil Research Institute, Toronto Western Hospital, Toronto, Ontario, Canada

ARTICLE INFO

Article history:
Received 18 May 2017
Accepted 14 June 2017
Available online 1 July 2017

Keywords:
Parkinson's disease
Virally over-expressing mutant α-synuclein rat
Neuroprotection
Substantia nigra
Mitochondria
Sirtuin 3

ABSTRACT

Parkinson's disease (PD) is a neurodegenerative movement disorder, which affects approximately 1–2% of the population over 60 years of age. Current treatments for PD are symptomatic, and the pathology of the disease continues to progresses over time until palliative care is required. Mitochondria are key players in the pathology of PD. Genetic and *post mortem* studies have shown a large number of mitochondrial abnormalities in the substantia nigra pars compacta (SNc) of the parkinsonian brain. Furthermore, physiologically, mitochondria of nigral neurons are constantly under unusually high levels of metabolic stress because of the excitatory properties and architecture of these neurons. The protein deacetylase, Sirtuin 3 (SIRT3) reduces the impact subcellular stresses on mitochondria, by stabilising the electron transport chain (ETC), and reducing oxidative stress. We hypothesised that viral overexpression of myc-tagged SIRT3 (SIRT3-myc) would slow the progression of PD pathology, by enhancing the functional capacity of mitochondria. For this study, SIRT3-myc was administered both before and after viral induction of parkinsonism with the AAV-expressing mutant (A53T) α-synuclein. SIRT3-myc corrected behavioural abnormalities, as well as changes in striatal dopamine turnover. SIRT3-myc also prevented degeneration of dopaminergic neurons in the SNc. These effects were apparent, even when SIRT3-myc was transduced after the induction of parkinsonism, at a time point when cell stress and behavioural abnormalities are already observed. Furthermore, in an isolated mitochondria nigral homogenate prepared from parkinsonian SIRT3–myc infected animals, SIRT3 targeted the mitochondria, to reduce protein acetylation levels. Our results demonstrate that transduction of SIRT3 has the potential to be an effective disease-modifying strategy for patients with PD. This study also provides potential mechanisms for the protective effects of SIRT3-myc.

1. Introduction

Parkinson's disease (PD) is a common neurodegenerative disease, the incidence of which will quadruple in the next twenty-five years. Current therapies treat parkinsonian symptoms, but have no impact on disease progression. When diagnosed with PD, patients are relatively mobile and independent. As the disease progresses, symptoms become more disabling until eventually palliative care is required. If a disease-modifying agent were available that could be given to patients upon diagnosis, PD would not reach its advanced stages. This would allow patients to maintain a good quality of life, which given our aging population would also have significant socio-economic benefits.

Genetic studies have revealed mutations around 20 loci encoding at least 12 proteins linked with increased risk of PD. Whilst these proteins are associated with a variety of cellular processes, such as regulation of the ubiquitin proteasome system (UPS), lysosomal function and mitochondrial function and trafficking, all mutations impact mitochondrial function on some level. This is of particular importance in dopaminergic neurons of the substantia nigra pars compacta (SNc), as they are particularly susceptible to cellular stress, which is regulated by the mitochondria (Exner et al., 2012; Yong-Kee et al., 2012a; Surmeier et al., 2010; Chan et al., 2010; Pacelli et al., 2015; Surmeier, 2007). Studies in *post mortem* PD brains have shown that complex I of the electron transport

* Corresponding author.
E-mail address: jnash@utsc.utoronto.ca (J.E. Nash).
[1] These authors contributed equally to the work.
Available online on ScienceDirect (www.sciencedirect.com).

http://dx.doi.org/10.1016/j.nbd.2017.06.009
0969-9961/

chain (ETC) is underactive (Schapira et al., 1992) and that there is an increase in the number of mitochondrial mutations (Bender et al., 2006; Reeve et al., 2008), further supporting a central role of mitochondria in PD pathology.

Sirtuins (SIRTs) are a family of seven NAD(+)-dependent protein deacetylases and ADP ribosylases that have long been known for their cytoprotective and longevity-enhancing effects (Kyrylenko and Baniahmad, 2010). Whilst SIRTs are ubiquitously expressed throughout the body, each SIRT subtype exhibits restricted cellular distribution (Sidorova-Darmos et al., 2014). SIRTs 1, 6 and 7 are located in the nucleus, SIRT2 in the cytosol, and SIRTs 3–5 are located in mitochondria (Herskovits and Guarente, 2014; Herskovits and Guarente, 2013; Zhang et al., 2010; Lucking et al., 2000; Valente et al., 2004; Matsuda et al., 2010). Deacetylation of lysine motifs represents one of the major ways in which mitochondrial proteins regulate bioenergetics processes. Within the mitochondria, there are over 700 proteins with at least 2200 acetylation motifs (Nogueiras et al., 2012; Hebert et al., 2013). Approximately 65% of the mitochondrial proteome is acetylated at any given time (Nogueiras et al., 2012; Hebert et al., 2013). Studies in non-neuronal cells of SIRT3 knockout mice show that SIRT3 is the major regulator of mitochondrial acetylation (Herskovits and Guarente, 2014; Herskovits and Guarente, 2013). SIRT3-deficient cells display significantly more acetylated mitochondrial proteins, which has been linked with lower ATP levels (Ahn et al., 2008), increased oxidative damage (Someya et al., 2010), diminished activity of Complexes I—V of the mitochondria respiratory chain (Ahn et al., 2008; Bao et al., 2010; Kim et al., 2010), and increased opening of the mitochondrial permeability transition pores (mPTP) (Hafner et al., 2010). Thus, in non-neuronal cells, SIRT3 enhances beneficial metabolic and anti-oxidant processes through the stabilisation and augmentation of mitochondrial bio-efficiency, and the suppression of ROS production (Lombard et al., 2007; Burnett et al., 2011). The multi-faceted mitochondrial health–enhancing capabilities of SIRT3 make it extremely attractive as a therapeutic target in neurodegenerative diseases, however, relatively few SIRT3 studies have been carried out in neuronal cells, and less than a handful were performed *in vivo*. Recent studies have shown that SIRT3 is neuroprotective in cell culture models of stroke, Huntington's disease and Alzheimer's disease (Dai et al., 2017; Fu et al., 2012; Weir et al., 2012). Furthermore, deletion of SIRT3 increases the sensitivity of dopaminergic neurons to MPP+ or DJ-1 knock-out (Liu et al., 2015; Shi et al., 2017). However, despite reports of the beneficial effects of SIRT3, other studies in stroke have shown that lack of SIRT3 is neuroprotective (Novgorodov et al., 2016). The aim of the current study was to validate ectopic introduction of SIRT3 as a disease–modifying agent in parkinsonism.

In the current study, we employed the adeno-associated virus (AAV) over-expressing human mutant α-synuclein (A53T) rat model of parkinsonism, as this model shows the progressive appearance of rodent equivalents of important markers for PD in patients. Three weeks post-transduction of A53T, α-synuclein-positive aggregates are present, and animals show asymmetries in forelimb use. After six weeks, there is also significant loss of dopaminergic neurons in SNc (Koprich et al., 2010; Koprich et al., 2011). Thus, the A53T rat is an excellent model for testing potential disease-modifying agents. In this study, we used a recombinant AAV (rAAV) to overexpress myc-tagged SIRT3. We show that SIRT3-myc is both neuroprotective and neurorestorative in parkinsonian rats. We also demonstrate target engagement and define a potential mechanism of action for SIRT3-myc, using a complement of biochemical and cell culture techniques.

2. Materials and methods

2.1. Vectors

For synthesis, rAAV expressing human A53T α-synuclein (accession number P37840, Variant ID VAR_007454) was inserted into a chimeric vector, comprised of equal parts AAV1 and AAV2 (Koprich et al., 2010; Koprich et al., 2011). SIRT3^{H248Y} (Shimazu et al., 2010) was kindly donated by Dr. Eric Verdin (UCSF, USA). Myc-tagged SIRT3^{H248Y} was synthesised by double restriction enzyme digestion of SIRT3^{H248Y} plasmid with *Bgl*II and *Pst*I. The fragment containing the H248Y mutation was then inserted into the SIRT3-myc plasmid, digested with the same restriction enzymes as was used to insert SIRT3. Insertion of SIRT3-myc (accession number Q9NTG7) and SIRT3^{H248Y}-myc into AAV1 serotype was driven by a chicken β-actin promoter. The SIRT3 wild-type and mutant vectors were produced by the Penn State vector core facility (Pennsylvania, USA). For studies using AAVs, empty vector (EV) was used as a control. Regarding controls for both mutant (A53T) α-synuclein and SIRT3-myc, the capsid of the EV was identical to that used to create each of the non-control AAVs. Thus, as a control for mutant (A53T) α-synuclein, the chimeric AAV1/2 vector was used. As a control for SIRT3-myc, an empty serotype 1 carriage was used.

2.2. Animals and vector delivery

The overall design of the studies involving A53T transgenic animals is shown in Fig. 1. Male and female Sprague Dawley rats (250–300 g) (Charles River, Canada) were housed in pairs in a temperature-controlled environment on a 12-hour light/dark cycle. Food and water were given *ad libitum*, except immediately prior to behavioural assessment, as described below. All procedures were conducted under the approval of the Animal Care Committees of the University of Toronto in accordance with the guidelines and regulations set by the Canadian Council on Animal Care. AAVs were delivered to the substantia nigra (SN) using stereotaxic surgery (coordinates: AP −5.2 mm, ML −2.0 mm, DB −4.5 mm from Bregma) (Paxinos and Watson, 1998). AAVs were infused at a rate of 0.2 μL/min (final volume 2 μL) using a microinjector (Stoelting). Following completion of the SIRT3 optimisation study, 2.59×10^{11} GC/mL of AAV SIRT3-myc or AAV SIRT3^{H248Y}-myc was delivered resulting in a final concentration of 5.18×10^{8}. For AAV A53T, 2.55×10^{12} GC/mL was infused into the SN, resulting in a final concentration of 5.1×10^{9} GC, as had been used previously (Koprich et al., 2010; Koprich et al., 2011). Animals were excluded from the groups if they did not show expression of the A53T and/or SIRT3-myc in the SN, as assessed by immunohistochemistry. Following exclusions, animal numbers ranged from 8 to 20 animals/group for behavioural analysis.

2.3. Cylinder (forelimb asymmetry) test

Six weeks following A53T or EV administration, forelimb asymmetry was assessed using the cylinder test (Whishaw and Kolb, 2005). To increase exploratory behaviour during the testing period, rats were deprived of food on the evening preceding the assessment. The following morning, rats were placed in a glass cylinder (19.2 cm diameter, 30.7 cm height) in front of two mirrors and were video recorded. The use of the right, left, and both paws against the cylinder wall for the first 20 contacts was recorded. Three consecutive trials were completed. Videos were scored *post hoc* by an independent observer blinded to the treatment conditions. The final data are presented as percent asymmetry [(% ipsilateral paw use − % contralateral paw use) / (% ipsilateral paw use + % contralateral paw use)] × 100.

2.4. Post-mortem analysis

Six weeks following A53T or EV infusion, animals were transcardially perfused with ice-cold 1× PBS under isoflurane/oxygen anaesthetic. Brains were removed and prepared for immunohistochemistry, HPLC or SDS-PAGE and Western blotting as described below.

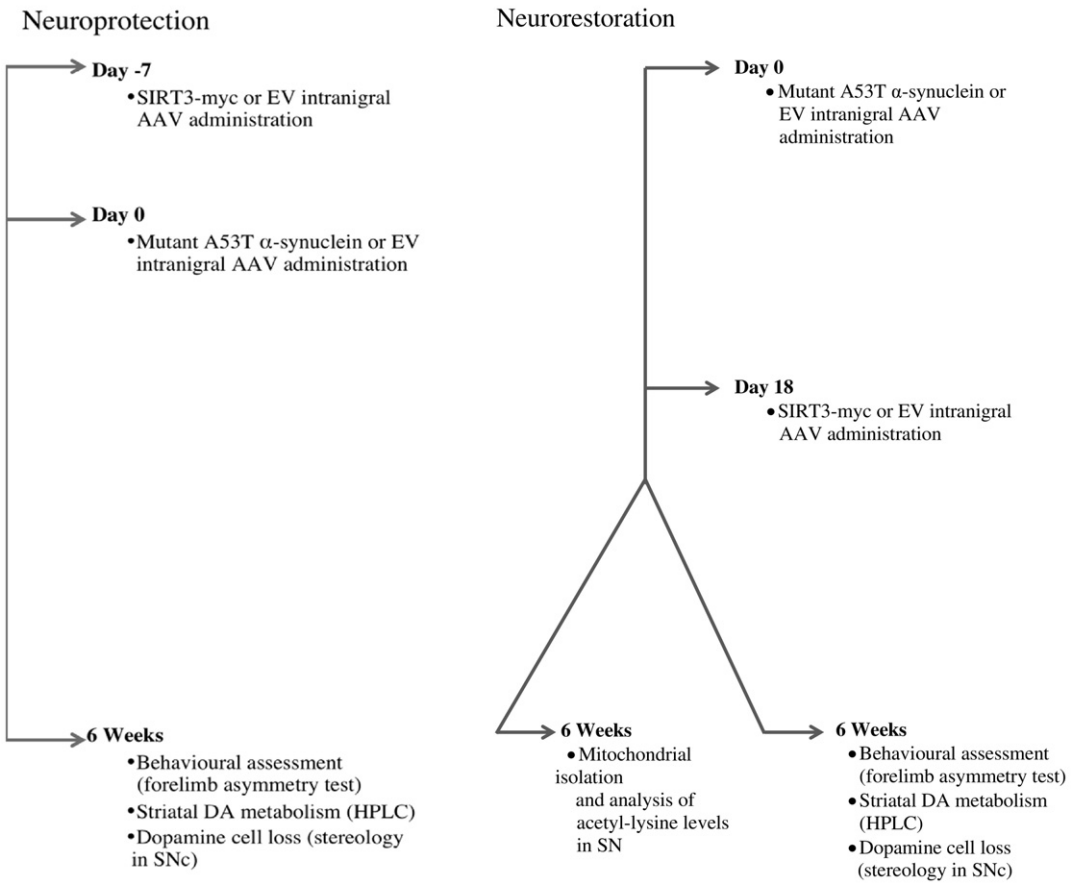

Fig. 1. Schematic to show study timelines for rAAV expressing animals. Methods performed at each time point are described.

2.5. Immunohistochemistry

For details of the antibodies used, see Table 1. The brain posterior to the striatum was post-fixed in 4% PFA, cryosectioned (40 μm thickness), and stored in cryoprotectant (30% glycerol, 30% ethoxyethanol, 40% PBS) for immunohistochemistry.

For immunofluorescence, sections were washed in PBS containing 0.1% Triton X-100 (PBS-T), blocked for 1 h in 5% normal goat serum (NGS) in PBS-T and incubated overnight in primary antibody (4 °C). Sections were then washed in PBS-T, and incubated for 3 h in secondary antibody protected from light. Following washes in PBS, sections were annealed onto Superfrost slides (VWR) and allowed to dry protected from light. Once dry, the slides were washed in ddH_2O and mounted with fluorescence mounting medium (Dako).

For colorimetric staining, sections were washed in PBS-T, and endogenous peroxidase was quenched with 3% hydrogen peroxide. Sections were then washed in PBS-T and blocked for 1 h in 5% NGS in PBS-T before being incubated overnight with NeuN antibody (4 °C). After washing in PBS-T, the tissue was incubated for 2 h with a biotinylated secondary antibody and subsequently in Elite avidin-biotin complex (ABC kit, Vector Labs) for 1 h. Sections were then washed in PBS and reacted with 3,3-diaminobenzidine (DAB) (Vector Labs) for visualisation. Next, tissue was washed in PBS-T and incubated overnight with tyrosine hydroxylase (TH) antibody (4 °C) and subsequently washed in TBS with 0.1% Tween 20 (TBS-T). Sections were then incubated with an alkaline phosphatase conjugated secondary antibody and washed in TBS-T. Visualisation of the immunostaining was achieved using the Vector Blue kit (Vector Labs). The tissue was washed in PBS and annealed onto Superfrost slides and allowed to dry. Once dry, sections were hydrated in ddH_2O, with subsequent dehydration in an ethanol series (70%, 95%, 100%) and cleared using Histoclear (National Diagnostics) before being mounted using Vectamount (Vector Labs).

2.6. Stereology

The estimated number of dopaminergic neurons was quantified using unbiased stereological methods. TH-stained sections of the SN were counted in a blinded fashion using an optical fractionator (Stereo Investigator (MBF Biosciences)). The medial, compacta, and lateral regions of the SN were counted in 240 μm gaps (1:6 series). The user defined SN at 5× magnification was divided by the program into 120 μm × 90 μm counting grids, with a 60 μm × 60 μm counting frame and 2 μm guards. Counting sites were analysed sequentially using a 100× oil immersion lens in the order set by the program to cover the entire SN, and the user evaluated tissue thickness at counting sites containing TH positive cells. All reported values represent the *estimated population using number weighted section thickness*. Sections were included in the study when the Schmitz-Hof coefficient of error (second estimate) was <0.1.

2.7. Catecholamine quantification using HPLC

Striatal sections were homogenised in trichloroacetic acid (TCA) (0.01 M sodium acetate, 0.0001 M EDTA, 5 ng/mL isoproterenol, 10.5% methanol). For quantification of dopamine and dopamine metabolites, striatal samples were sent to CMN/KC Neurochemistry Core Lab (Vanderbilt University, USA) for HPLC analysis. The homogenate was centrifuged and the supernatant analysed for biogenic amines using an Antec Decade II electrochemical detector operated at 33 °C and a C_{18}HPLC column (100 × 4.60 mm). Biogenic amines were eluted with a mobile

Table 1
Antibodies used for immunohistochemistry and Western blot. KEY: IH: immunohistochemistry, WB: Western blot.

Antibody	Source	Dilution
Acetyl-lysine (mouse)	Cell signaling (9441S)	1:1000
β-Actin (mouse)	Sigma Aldrich (A5441)	1:5000 (WB)
myc (mouse)	Cell signaling (2276S)	1:2000 (IH)
		1:1000 (WB)
myc (chick)	Life technologies (A-21281)	1:2500 (IH)
NeuN (mouse)	Millipore (MAB377)	1:1000 (IH)
NeuN (rabbit)	Chemicon (ABN78)	1:1000 (IH)
SIRT3 (rabbit)	Cell signaling (2627S)	1:1000 (WB)
α-Synuclein (mouse)	Invitrogen (32-8100)	1:500 (IH)
TOM20 (rabbit)	Santa Cruz (Sc-11415)	1:5000 (IH)
		1:500 (WB)
Tyrosine hydroxylase (mouse)	Immunostar (22941)	1:1000
Tyrosine hydroxylase (rabbit)	Millipore (AB152)	1:2000 (IH)
		1:1000 (WB)
Goat anti-rabbit biotinylated	Vector (BA-1000)	1:400 (IH)
Goat anti-mouse biotinylated	Vector (BA-9200)	1:400 (IH)
Alexafluor 488 (goat anti-chick)	Jackson (111-585-144)	1:500 (IH)
Alexafluor 647 (goat anti-mouse)	Jackson (115-605-146)	1:500 (IH)
Alexafluor 594 (goat anti-rabbit)	Jackson (115-545-003)	1:500 (IH)
Alkaline phosphatase (goat anti-rabbit)	Vector Labs (111-055-003)	1:250 (IH)
Alkaline phosphatase (goat anti-mouse)	Jackson (115-055-166)	1:250 (IH)
Goat anti-rabbit HRP	BioRad (A6154)	1:5000 (WB)
Goat anti-rabbit HRP	Jackson (111-035-144)	1:5000 (WB)

phase (89.5% 0.1 M TCA, 0.01 M sodium acetate, 0.0001 EDTA, and 10.5% methanol, pH 3.8).

2.8. Isolation of mitochondria

Mitochondria from the right SN of each animal were isolated using a protocol adapted from Chinopoulos et al. (2011). Brain tissue of the right SN was homogenised in 1 mL of MGSEGTA-BSA (225 mM mannitol, 75 mM sucrose, 5 mM HEPES (pH 7.4), 1 mM EGTA, dissolved in water) with a 1 mL hand-held homogenizer for 35 strokes. The homogenate was then transferred into two 1.5 mL tubes, which was topped up with MSEGTA-BSA to the inner groove to yield ~1.5 mL of total volume, then mixed by inversion. The tubes were then centrifuged at ~500*g* for 5 min, after which the supernatant was transferred into clean 1.5 mL tubes and centrifuged (14,000*g* × 10 min). The supernatant was discarded, and the pellet resuspended in 0.2 mL of 12% Percoll-MSEGTA (100% Percoll™-MSEGTA buffer: 225 mM mannitol, 75 mM sucrose, 5 mM HEPES (pH 7.4), 1 mM EGTA, dissolved in 100% Percoll™ and diluted to 12% using MSEGTA: 225 mM mannitol, 75 mM sucrose, 5 mM HEPES (pH 7.4), 1 mM EGTA, dissolved in H_2O). This combined fraction was layered over 1 mL of 24% Percoll-MSEGTA in a clean 1.5 mL tube and centrifuged (18,000*g* × 15 min). The top 0.5 mL portion of the sample was aspirated and saved as the cytosolic fraction, 1 mL of MSEGTA was added, mixed by inversion, and centrifuged (18,000*g* × 5 min). The pellet was resuspended in buffer, and 1.3 mL of MSEGTA added and mixed by inversion before centrifugation (14,000*g* × 5 min). The supernatant was then discarded, and the pellet was resuspended in 0.1 mL of MSEGTA to yield the final solution containing the purified mitochondria.

2.9. SDS-PAGE and Western blot analysis

Samples were prepared in 11.25 μL of 4× Laemmli Sample Buffer (BIO-RAD) and the appropriate volume of 1× Tris Buffered Saline (TBS) was added to yield 30 μg of protein in a total volume of 45 μL. The samples were loaded into a 10% acrylamide gel along with 5 μL of BLUeye Prestained Protein Ladder. The gels were run at 65 V through the stacking layer, then 125 V through the separating layer. Following transfer and blocking, primary antibodies were incubated overnight at 4 °C. See Table 1 for a detailed description of the antibodies used for this study. Images of blots were taken using Image Lab (BIO-RAD) software and analysed using ImageJ.

2.10. Generation of primary neuronal cultures

Cultures were prepared according to a previously described protocol (Fasano et al., 2008), with minor variations. Dissociated neurons, microdissected from the SN of postnatal day 0–2 (P0–P2) C57BL6 mice were seeded on a monolayer of corresponding cortical astrocytes, grown on collagen/poly-L-lysine-coated glass coverslips. The total seeded neuron density was 250,000 cells/mL. All cultures were incubated at 37 °C in 5% CO_2 and maintained in 2/3 of Neurobasal™-A medium enriched with 1% penicillin/streptomycin, 1% Glutamax™-1, 2% B-27 supplement, and 5% fetal bovine serum (Life Sciences) plus 1/3 of minimum essential medium (MEM) enriched with 1% penicillin/streptomycin, 1% GlutamaxTM-1, 20 mM Glucose, 1 mM sodium pyruvate, and 100 μL MITO + serum-extender.

2.11. Metabolic flux experiments in primary cultured neurons

The rate of oxygen consumption deriving from mitochondrial OXPHOS was assessed using an extracellular flux analyzer (Seahorse Biosciences), as previously described (Pacelli et al., 2015). Cells were plated on XF24 tissue culture plates, infected with AAV1 expressing human SIRT3-myc (1 μL/mL) and maintained in culture for 10 days. Before experiments, cells were incubated for 1 h at 37 °C in a CO_2-free incubator in bicarbonate-free DMEM (Sigma) supplemented with 200 mM GlutaMax™-1 (Life Sciences), 100 mM sodium pyruvate (Sigma), 25 mM D-glucose (Sigma), 63.3 mM NaCl (Sigma) and phenol red (Sigma), with pH adjusted to 7.4 with NaOH. Oxygen consumption was sequentially measured under basal conditions in the presence of the mitochondrial uncoupler CCCP (0.5 μM) to assess the maximal oxidative capacity, and in the presence of the mitochondrial inhibitors rotenone (1 μM) and antimycin A (1 μM) to assess non-mitochondrial oxygen consumption. After the assays, the cells were immediately fixed for immunofluorescence. Since neurons were cultured together with astrocytes, parallel measurements were also performed from pure astrocyte cultures and the OCR values subtracted from those of mixed cultures.

2.12. Mitochondrial function measurement in SH-SY5Y cells

Human neuroblastoma catecholaminergic, undifferentiated SH-SY5Y cells (CRL-2266, ATCC, USA) were stably transfected with pLKO-myc or pLKO-SIRT3-myc using Lipofectamine 2000 (Invitrogen). Cells were cultured in Dulbecco's Modified Eagle's Medium (DMEM) (Wisent, Canada) containing 4.5 g/L glucose, L-glutamine, and sodium pyruvate with 10% bovine serum albumin (BSA) (Wisent, Canada) and 5 μM Blasticidin S (Enzo Life Sciences).

2.12.1. Cell viability and cell death assays

Cell viability and cell death was assessed using Alamar Blue and propidium iodide (PI) (both from Life Sciences) respectively. SH-SY5Y-myc and SH-SY5Y-SIRT3-myc cells were plated at 1×10^5 cell/mL. To measure viability, cells were exposed to approximate [IC_{50}] of rotenone (30 nM), dopamine hydrochloride (65 μM), naphthazarin (5,8-dihydroxy-1,4-napthoquinone) (300 nM), (all from Sigma) or PSI (Z-Ile-Glu(Obu^t)-Ala-Leu-H) (Biolynx, USA) (30 nM) with Alamar Blue (10% of final volume) for 24 h. Fluorescence was measured at 530 nm excitation and 590 nm emission. To measure cell death, cells were exposed to the toxins listed above. Following a 24-hour incubation, cells were incubated with 2 μM of PI for 1 h prior to quantification by fluorescence measurement (excitation 535 nm, emission 617 nm).

2.12.2. Reactive oxygen species measurement

ROS was measured using CM-H_2DCFA (2′7′-dichlorodihydrofluorescein diacetate) according to the manufacturer's instructions (Invitrogen). Briefly, SH-SY5Y-myc and SH-SY5Y-SIRT3-myc cells were plated at 2.5×10^5 cell/mL. Cells were exposed to rotenone, dopamine hydrochloride, naphthazarin, or PSI for 24 h and subsequently washed with DMEM without phenol red and treated with CM-H_2DCFDA (10 μM) for 30 mins in the dark. Following this, cells were washed with DMEM without phenol red and ROS was measured using flow cytometry (BD LSRFortessa).

2.12.3. Quantification of ATP levels

ATP was quantified using the ViaLight™ HS kit (Lonza) according to the manufacturer's instructions. Briefly, SH-SY5Y-myc and SH-SY5Y-SIRT3-myc cells were plated at 1×10^5 cell/mL. Cells were exposed to rotenone, dopamine, napthazarin, or PSI for 24 h. 100 μL of nucleotide releasing reagent was added to each well and incubated for 5 min. Subsequently, 20 μL of ATP monitoring reagent was added and luminescence readings were obtained.

2.13. Statistical analysis

One-way ANOVA with Tukey *post hoc* was used for AAV optimisation and behavioural studies, stereological and non-stereological cell counting, and HPLC. For isolated mitochondria studies, a Mann-Whitney *U* test was used to analyse the Western blots, and the Spearman correlation nonparametric test was used to determine correlation between limb use, SIRT3-myc expression and acetylation levels (Fig. 6). A student two-tailed *t*-test was used for mitochondrial bioenergetics studies in cultured dopaminergic neurons. For SH-SY5Y studies, ANOVA, using vector expressed and treatment as the two variables, with Tukey *post hoc* was used. For behavioural, HPLC, and stereology studies in Figs. 3 and 4, outliers were identified using a Grubbs test (alpha = 0.05). For Western blot analysis in Fig. 6, outliers were identified using median absolute deviation (Leys et al., 2013). Statistical analysis was performed using GraphPad Prism 6.0.

3. Results

3.1. Optimisation of SIRT3-myc AAV infection in vivo

To reduce the chance of a false-negative result, we first optimised the delivery of myc-tagged SIRT3 AAV1. The optimal titre was defined as that which caused no change in neuronal number, dopaminergic phenotype or endogenous SIRT3 levels, whilst increasing SIRT3-myc > 2-fold above endogenous levels of SIRT3, with no SIRT3-myc expression on the contralateral (uninjected) hemisphere. Titres (3.37, 5.18, 6.74 and 22.50×10^8 GC) of rAAV SIRT3-myc were infused into the SN. Fourteen days later, brains were removed and analysed using SDS-PAGE with Western blot or immunohistochemistry. Following infection with rAAV SIRT3-myc, SIRT3-myc was highly expressed in the SN ipsilateral to the injection site at all titres tested, showing around 150% above loading control for 3.37, 5.18, 6.74 and 22.50×10^8 GC of rAAV SIRT3-myc respectively, with little expression in the contralateral hemisphere (Fig. 2 Ai). SIRT3-myc had no significant effect on endogenous SIRT3 levels, with optical density (OD) ranging between 30 and 46 AU of loading control, which was comparable to endogenous SIRT3 in naïve animals (45 AU) (Fig. 2 Aii). All titres of rAAV SIRT3 caused SIRT3-myc levels to be at least 3-fold higher than endogenous SIRT3 (Fig. 2 Aiii). At the concentration range tested, rAAV SIRT3-myc had no significant effect on the number of NeuN-positive cells in the SN (Fig. 2B). Following infection in the SN, SIRT3-myc expression was also observed throughout the striatum (Fig. 2C). A final concentration of 5.18×10^8 GC was chosen, as it met all our criteria for optimal titre. This titre is comparable to previous studies using AAV1 in the rat SN (McFarland et al., 2009). This titre infected approximately 90% of all cells within the SN.

Next we determined whether SIRT3-myc transduction was stable over time. Three days following rAAV infusion, SIRT3-myc was highly expressed in the SN, and remained stable for 84 days (Fig. 3A). There was no loss of dopaminergic phenotype over this time period (Fig. 3B), confirming that 5.18×10^8 GC is an appropriate concentration for our studies.

3.2. SIRT3-myc overexpression is neuroprotective in the mutant A53T synuclein rat

The overall design of the studies involving A53T rats is shown in Fig. 1. For the neuroprotection arm of the study, 7 days prior to unilateral injection of A53T in the SN, AAV SIRT3-myc or empty vector (EV) was infused at the identical injection site. Six weeks following A53T infusion (A53T + EV), there was 33.41 ± 6.83% asymmetry in forelimb use between the parkinsonian and unaffected limb, compared to 1.92 ± 5.33% in the EV + EV group (Fig. 4A), which is comparable to the percentage asymmetry observed previously in this model (Koprich et al., 2010; Koprich et al., 2011). Six weeks following A53T transduction, there was also a 46% decrease in TH-positive cell number in the SN, compared to the EV + EV group (Fig. 4B). Also, there was a 135.2% and 143.8% increase in HVA/DA and DOPAC/DA ratios respectively compared to the uninjected hemisphere (Fig. 4D,E), suggesting increased DA turnover. When SIRT3 was infused 7 days prior to A53T, A53T-induced parkinsonian symptoms and pathology was prevented, such that there was no limb-use asymmetry (Fig. 4A), no loss of dopaminergic neurons (Fig. 4B), and no change in striatal dopamine metabolism (Fig. 4C–E).

3.3. SIRT3-myc has restorative effects in the mutant A53T synuclein rat

Next we addressed whether SIRT3-myc could rescue neurons undergoing stress in A53T transduced rats, by administering SIRT3-myc 18 days following A53T infusion. Six weeks following A53T transduction (A53T + EV group), forelimb asymmetry (35.58 ± 5.62%) (Fig. 5A), loss in TH-positive cell number (41%) (Fig. 5B), and changes in striatal dopamine metabolism (Fig. 5C–E) were comparable to those observed in the neuroprotection study. Transduction of SIRT3-myc on day 18 reversed motor deficits, such that limb-use was comparable to control (EV + EV: 9.72 ± 4.83% asymmetry compared to A53T + SIRT3-myc: 11.75 ± 4.64% asymmetry) (Fig. 5A). SIRT3-myc also prevented loss of TH-positive cells (EV + EV: 3820 ± 306 cells compared to A53T + SIRT3-myc: 5684 ± 578 cells) (Fig. 5B). Finally, SIRT3-myc also reversed A53T-induced changes in striatal DA turnover, restoring striatal DA metabolism to control (EV + EV) levels (Fig. 5C–E). In A53T animals, the deacetylase inactive SIRT3 AAV (AAV SIRT3^{H248Y}-myc) had no effect on limb use or nigral dopamine cell number compared to control-treated, parkinsonian (A53T + EV) animals (A53T + SIRT3^{H248Y}-myc: 39.99 ± 9.23% asymmetry; 2987 ± 309.3 cells) (Fig. 5A,B). However, there was a significant difference between loss of TH cell number in the A53T + SIRT3^{H248Y}-myc group compared to the A53T + SIRT3 group (Fig. 5B). Whilst there was no significant difference in limb-use asymmetry between the SIRT3-myc and SIRT3^{H248Y}-myc groups, the *p* value from *post-hoc* analysis was close to significant ($p = 0.06$).

3.4. SIRT3-myc is a mitochondrial protein deacetylase

To address whether myc-tagged SIRT3 functioned in the same way as endogenous SIRT3 *in vivo*, we addressed whether SIRT3-myc targeted the mitochondria and regulated mitochondrial acetyl-lysine levels. Following nigral injection of A35T and SIRT3-myc/EV, brains were removed and immunohistochemistry performed. SIRT3-myc co-localised with the mitochondrial protein TOM20 in both dopaminergic and non-dopaminergic cells of the SN (Fig. 6A).

Endogenous SIRT3 is synthesised in the nucleus in its long form, which is a 44 kDa protein with a mitochondrial targeting sequence

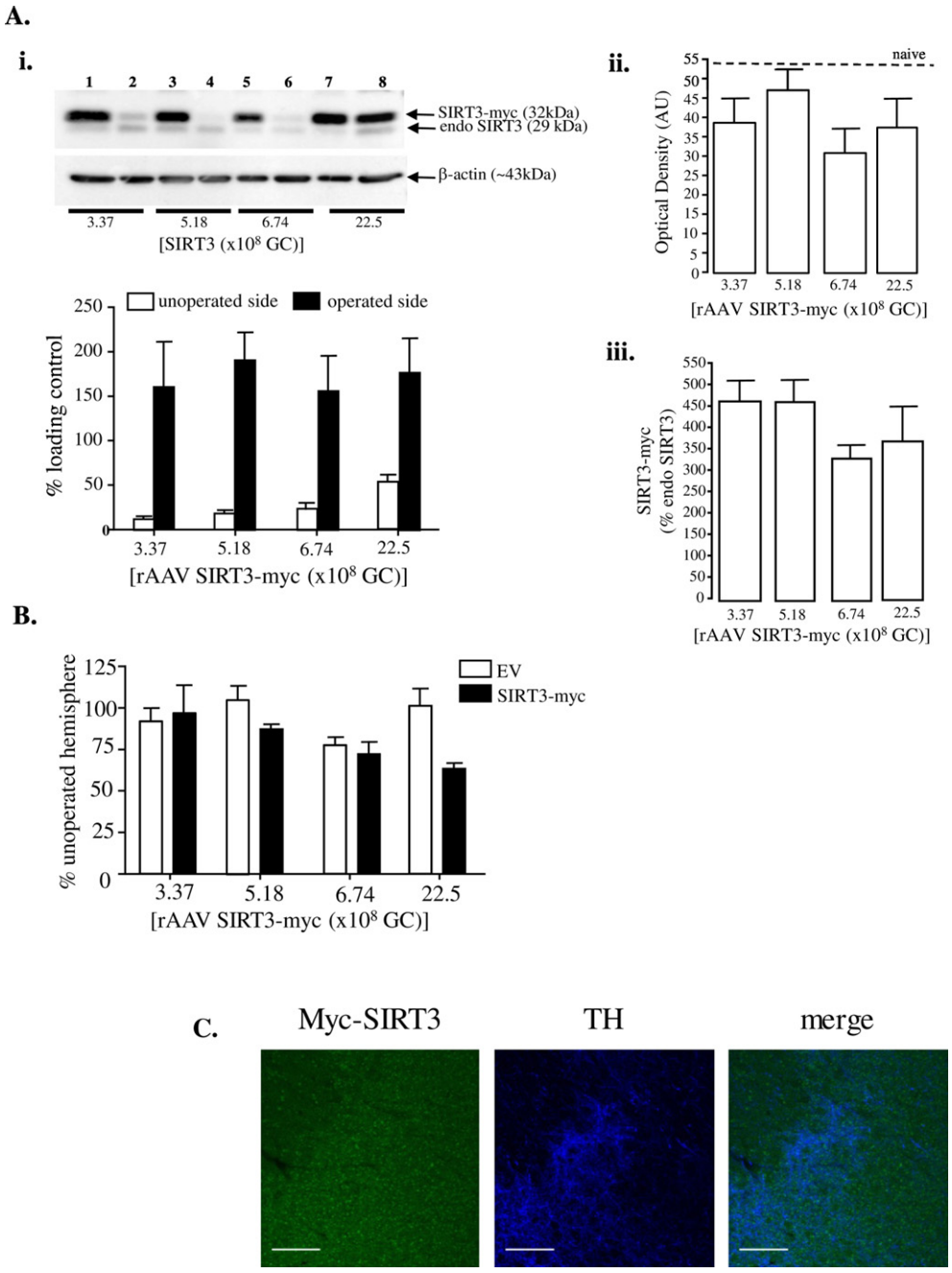

Fig. 2. Optimisation of titre for viral over-expression of SIRT3-myc in the substantia nigra. Rats were intra-nigrally infused with rAAV expressing SIRT3-myc at concentrations 3.37, 5.18, 6.74 and 22.5 × 10^8 GC for 2 weeks. Nigral levels of SIRT3-myc, endogenous SIRT3 and NeuN were quantified using SDS-PAGE and Western blot or immunohistochemistry. Ai. Expression of SIRT3-myc and endogenous SIRT3. Blots show SIRT3-myc (32 kDa) and endogenous SIRT3 (29 kDa) expression in operated (lanes 1, 3, 5, 7, 8) and unoperated (lanes 2, 4, 6) hemispheres. Graph shows mean SIRT3-myc expression as a percentage of loading control (β-actin) ± SEM ($n = 5$). Aii. Effect of SIRT3-myc over-expression on endogenous SIRT3 levels. Graph shows mean endogenous SIRT3 optical density (OD) as a percentage of loading control (β-actin) ± SEM from the blots in figure 2Ai ($n = 5$). The dotted line represents levels of endogenous SIRT3 in naïve animals. Aiii. Expression of SIRT3-myc compared to endogenous SIRT3. Data are expressed as mean ± SEM percentage SIRT3-myc OD compared endogenous SIRT3 OD. B. Effect of SIRT3-myc on NeuN counts. To assess the number of viable cells, sections were immunostained for NeuN. NeuN was counted at two different levels in the SN and is expressed as a percentage of NeuN in the unoperated SN. Values are presented as mean ± SEM ($n = 5$). C. SIRT3-myc expression in the striatum. Immunohistochemistry was performed on striatal sections ipsilateral to SIRT3-myc AAV infusion using antibodies against myc (green) to label SIRT3-myc expression and tyrosine hydroxylase (TH) to label dopaminergic fibres (blue). Scale bar = 100 μm.

(MTS). It is then transported to the mitochondria, where the MTS is cleaved, producing the short (28 kDa), active form to serve as a mitochondrial deacetylase (Shulyakova et al., 2014; Scher et al., 2007; Shi et al., 2005). We assessed whether SIRT3-myc showed the same characteristics in parkinsonian rats. Following *in vivo* administration of A53T and SIRT3-myc, the nigra was dissected, mitochondrial fraction isolated, then SIRT3 and acetyl-lysine levels quantified using Western blot. TOM20 was expressed exclusively in the mitochondrial fraction with no expression in the cytosolic fraction indicating that the mitochondria had been successfully isolated (Fig. 6 Bi). We found that in the mitochondrial fraction, the short form of endogenous SIRT3 was expressed equally in the control (A53T + EV) and SIRT3 expressing groups, showing that over-expression of SIRT3-myc did not alter the expression of endogenous SIRT3, as was observed in whole tissue homogenates in Fig. 2. In the SIRT3-myc expressing group, there were two bands, with molecular weights 47 kDa and 31 kDa (Fig. 6 Bii). Since the myc tag

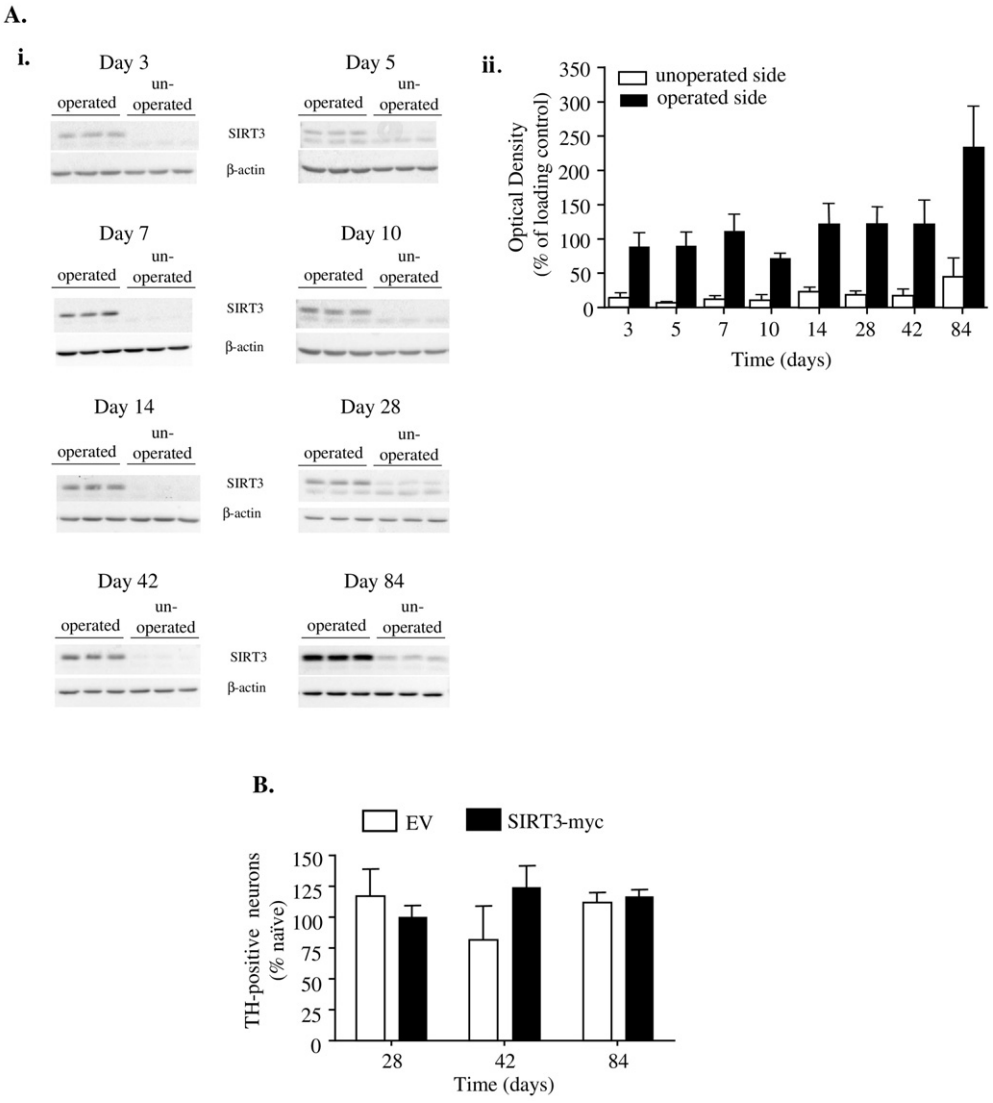

Fig. 3. Characterisation of the effect of chronic transduction of SIRT3-myc in the substantia nigra. On Day 0, rats were intra-nigrally infused with rAAV expressing SIRT3-myc or empty vector (EV) at a final titre of 5.0×10^8 GC. A. On days 3, 5, 7, 10, 14, 28, 42, and 84, nigral SIRT3 expression was measured by SDS-PAGE and Western blot ($n = 4$–6). (i). Blots to show endogenous SIRT3, SIRT3-myc, and the loading control β-actin expression. (ii) Graph to show mean ± SEM OD from the blots in 3Ai as a percentage of loading control (β-actin). ($n = 4$–6). B. Effect of SIRT3-myc over-expression on TH-positive cell counts in the SN. On days 28, 42, and 84, sections were immunostained for TH. The number of TH-positive neurons in the SN was determined using unbiased stereology and is expressed as a percentage compared to the number of neurons in naïve SN. Values are mean ± SEM ($n = 5$).

has a molecular weight of approximately 3 kDa, these bands likely represent the long and short form of SIRT3-myc respectively. Next we assessed levels of acetyl-lysine in the control (A53T + EV) and SIRT3-myc (A35T + SIRT3-myc) expressing groups using a pan acetyl-lysine antibody. Western blot showed five acetyl-lysine-positive bands at molecular weights ranging between 42 and 71 kDa (Supplementary Fig. 1A). Densiometric analysis of the bands showed that only two of these bands (57 kDa and 71 kDa) were significantly different in the SIRT3-myc expressing group compared to EV (Supplementary Fig. 1B). Thus, subsequent analysis focussed on the 57 and 71 kDa bands. In the control group (A53T + EV), levels of acetyl-lysine were almost 3-fold higher than in the SIRT3-myc group, suggesting that SIRT3-myc deacetylates lysine residues of mitochondrial proteins *in vivo* (Fig. 6 Biii).

To determine whether there was a correlation between SIRT3-myc expression and percentage limb-use asymmetry or acetyl-lysine levels in the mitochondria, the Spearman correlation nonparametric test was used. There was no correlation between SIRT3-myc levels, limb-use or acetylation levels.

3.5. In cultured dopaminergic neurons, SIRT3-myc enhances mitochondrial bioenergetics

Mitochondrial OXPHOS was assessed in primary cultures of dopaminergic neurons of mouse SN by measuring basal and maximal (uncoupled with CCCP) oxygen consumption rate (OCR) as described by Pacelli et al. (2015). We found that both basal and maximal OCR was reduced in nigral neurons expressing SIRT3 by approximately 40% and 70% respectively (Fig. 7A,B). This was accompanied in SIRT3-expressing cells by a small increase in the respiratory control ratio (RCR) (Fig. 7C), which is the ratio between basal and maximal OCR, suggesting the existence of an increased ability to produce ATP in response to cellular stress. Together these data suggest that SIRT3 causes an increase in mitochondrial efficiency in dopaminergic neurons, leading to increased resilience to stress. Finally, no change in glycolysis was observed in cells expressing SIRT3 compared to control (data not shown), indicating that decreased respiration rate in SIRT3-myc expressing cells was not due to a transfer of ATP producing pathways to anaerobic mechanisms.

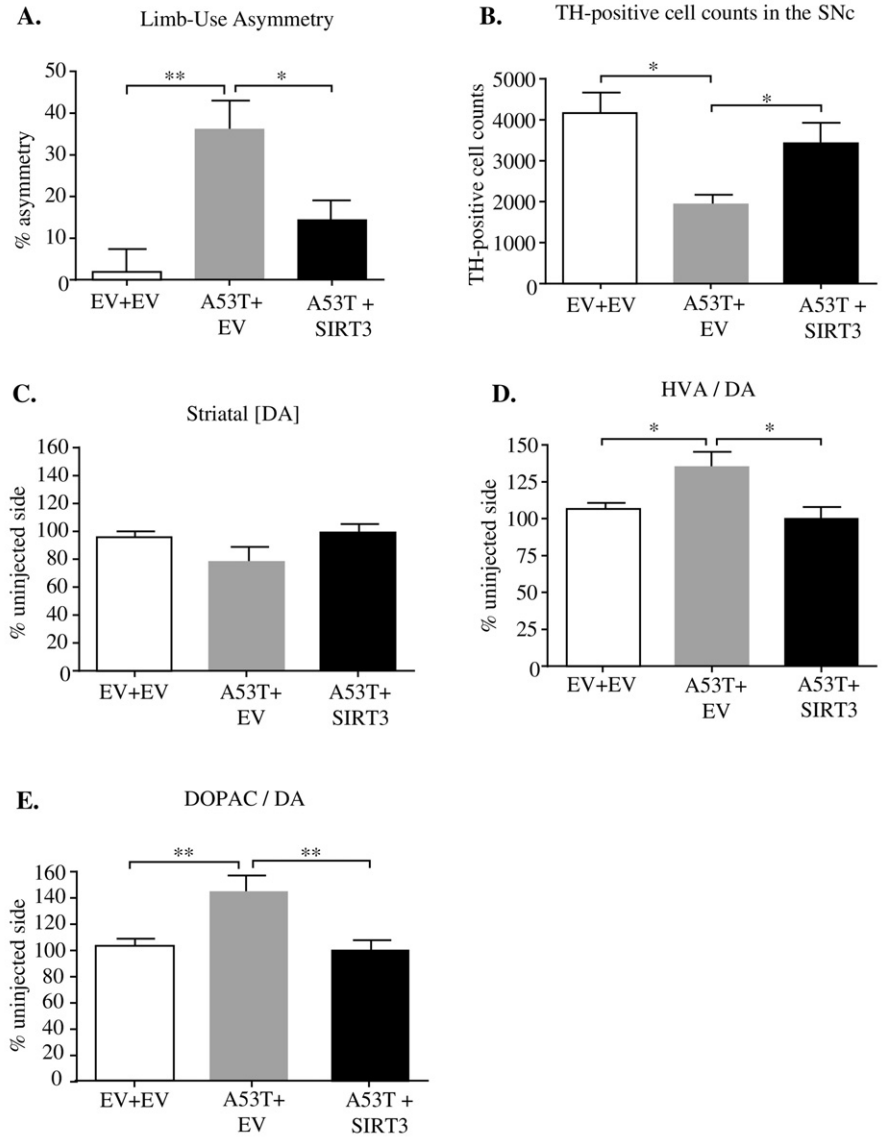

Fig. 4. SIRT3 is neuroprotective in the virally over-expressing mutant (A53T) α-synuclein rat model of parkinsonism. Seven days prior to administration of A53T AAV (defined as day minus 7), rats were intra-nigrally infused with rAAV SIRT3 or vehicle (EV). On day 0, rats were intra-nigrally infused with rAAV-A53T or vehicle (EV). A. Forelimb asymmetry. Six weeks following A53T injection, motor function was assessed using the cylinder test. Data are expressed as mean percentage forelimb limb asymmetry ± SEM. ANOVA: $F_{2,25} = 8.797$; $p = 0.001$, $n = 8, 10, 8$^. B. Stereological quantification of TH–positive neurons in the SNc. Data are expressed as mean TH-positive cell number in the SN ± SEM. The dotted line represents the number of TH-positive cells in the SN of a naïve animal. ANOVA: $F_{2,24} = 4.52$; $p < 0.022$, $n = 8, 10, 4$^. C–E. Assessment of dopamine (DA) turnover in the striatum using HPLC ($n = 7$–10). Levels of striatal DA, and DA metabolites (HVA and DOPAC) were measured in the hemisphere ipsilateral and contralateral to A53T AAV injections using HPLC. Data are expressed as mean percentage of the uninjected hemisphere ± SEM. C. Striatal dopamine. ANOVA: $F = 2.179$; $p_{2,23} = 0.136$, D. striatal HVA/DA. ANOVA: $F_{2,23} = 5.719$; $p = 0.010$; E. striatal DOPAC/DA. ANOVA: $F_{2,23} = 8.641$; $p = 0.002$. KEY: Tukey *post-hoc* $^*p < 0.05$, $^{**}p < 0.01$; ^number of replicates for groups EV + EV, A53T + EV, and A53T + SIRT3 respectively.

To further explore the potential mechanisms underlying the stabilising effect of SIRT3 on mitochondria bioenergetics, we used the catecholaminergic cell line, SH-SY5Y stably overexpressing SIRT3-myc or myc (control). Cells were exposed to toxins that mimic cell death processes linked with PD (Yong-Kee et al., 2011): rotenone (mitochondrial complex I inhibitor), dopamine (induces oxidative stress), naphthazarin (lysosome inhibitor), and PSI (ubiquitin-proteasome system inhibitor). Furthermore, these toxins cause mitochondrial dysfunction early in the cell death pathway in SH-SY5Y cells (Yong-Kee et al., 2012a; Yong-Kee et al., 2011). SIRT3-myc overexpression prevented toxin-induced decreases in cell viability and increases in cell death, demonstrating that SIRT3-myc is cytoprotective against a variety of PD-like insults in SH-SY5Y cells (Fig. 8A,B). We also assessed ROS levels using the dye CM-H_2DCFA. In control cells all toxins significantly increased ROS levels. SIRT3-myc overexpression reduced ROS by approximately 40% in basal conditions, and also inhibited toxin-induced increases in ROS (Fig. 8C). Finally, ATP levels were measured. In control (myc) cells, all toxins caused a significant decrease (approximately 45%) in ATP levels compared to vehicle (Fig. 8D). In vehicle-treated SIRT3-myc cells, ATP levels were significantly reduced compared to vehicle-treated myc cells. In SIRT3-myc cells, following exposure to toxins, there was no significant difference in ATP levels compared to myc cells, and also compared to the SIRT3-myc expressing, vehicle-treated group (Fig. 8D).

4. Discussion

The aim of this study was to validate the disease-modifying capacity of virally introduced SIRT3 in a rodent model of parkinsonism. Our optimisation studies showed that SIRT3-myc was highly expressed in the SN unilateral to the AAV injection, with no expression in the SN contralateral to the injection. Also, there was SIRT3-myc expression in the

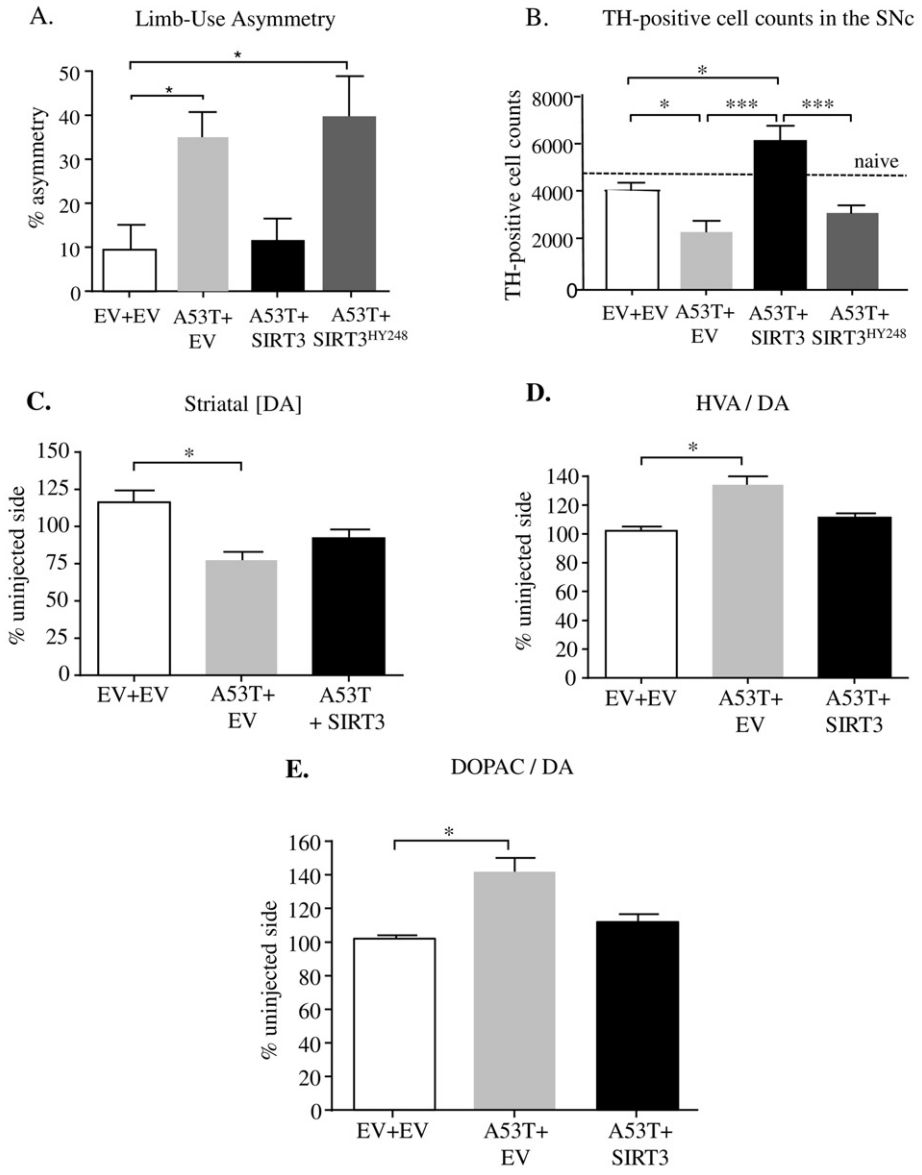

Fig. 5. SIRT3 is neurorestorative in the virally over-expressing mutant (A53T) α-synuclein rat model of parkinsonism. On day 0, rats received intra-nigral injections of rAAV-A53T or empty vector (EV). Eighteen days later, rats received intra-nigral injections of rAAV SIRT3-myc or EV. Six weeks following A53T injection and 24 days after SIRT3 injection, motor function was assessed using the cylinder test. Data are expressed as mean percentage forelimb limb asymmetry ± SEM. ANOVA: $F_{3,49} = 5.157$, $p = 0.0035$; $n = 12, 20, 10, 13$^. (B) Stereological quantification of TH–positive neurons in the SNc. Data are expressed as mean ± SEM. ANOVA: $F_{3,39} = 8.97$; $n = 12, 10, 10, 12$^. (C–E) Assessment of dopamine (DA) turnover in the striatum using HPLC ($n = 6, 14, 5$^). Levels of striatal DA and DA metabolites (HVA and DOPAC) were measured in the hemisphere ipsilateral and contralateral to the A53T injection using HPLC. Data are expressed as mean ± SEM percentage of the uninjected hemisphere (C) striatal dopamine levels. ANOVA: $F_{2,23} = 3.32$, $p = 0.036$, (D) striatal HVA/DA. ANOVA: $F_{2,24} = 3.832$; $p = 0.012$, (E) striatal DOPAC/DA. ANOVA: $F_{2,24} = 5.42$; $p = 0.114$. KEY: Tukey *post-hoc* $^*p < 0.05$, $^{***}p < 0.001$; ^number of replicates for groups EV + EV, A53T + EV, A53T + SIRT3, and A53T + $SIRT3^{HY248}$-myc respectively.

striatum, indicating that AAV SIRT3-myc is anterogradely transported along the nigrostriatal pathway, however, striatal SIRT3-myc expression was not quantified. Following optimisation and characterisation of AAV-SIRT3-myc transduction in the SNc, we assessed the effect of this vector, both before and after induction of parkinsonism. As a model of parkinsonism, we used the AAV over-expressing mutant (A53T) α-synuclein rat, which shows the progressive appearance of rodent equivalents of classic markers of PD observed in patients. Three weeks' post-transduction of A53T, α-synuclein-positive aggregates are evident, and there is marked forelimb asymmetry. After six weeks, there is significant loss of dopaminergic cells in SNc, and loss of TH-positive fibres in the striatum (Koprich et al., 2010; Koprich et al., 2011). Thus, this is an excellent model for testing potential disease-modifying agents. A tagged form of SIRT3, SIRT3-myc, was delivered using AAV1, which has a high transduction efficiency in dopaminergic neurons of the rat SNc (McFarland et al., 2009), and has also proved to be well tolerated and efficacious for gene delivery in clinical trials (Greenberg et al., 2016; Mendell et al., 2015). SIRT3-myc was protective, whether given to healthy cells prior to induction of parkinsonism, or after induction of parkinsonism, when there is evidence of cellular stress. In parkinsonian rats, SIRT3-myc corrected forelimb asymmetry, reversed changes in striatal dopamine metabolism, and prevented degeneration of dopaminergic neurons in the substantia nigra pars compacta (SNc). These effects seem to be dependent on the deacetylase abilities of SIRT3, since the deacetylase-deficient mutant construct had no effect on limb use asymmetry or dopamine cell number. We also show that ectopically-introduced SIRT3, targets mitochondria of nigral cells, where it has positive effects on bioenergetics. These effects are likely to reduce the susceptibility of this vulnerable population of neurons, thus alleviating mitochondrial stress to prevent neurodegeneration.

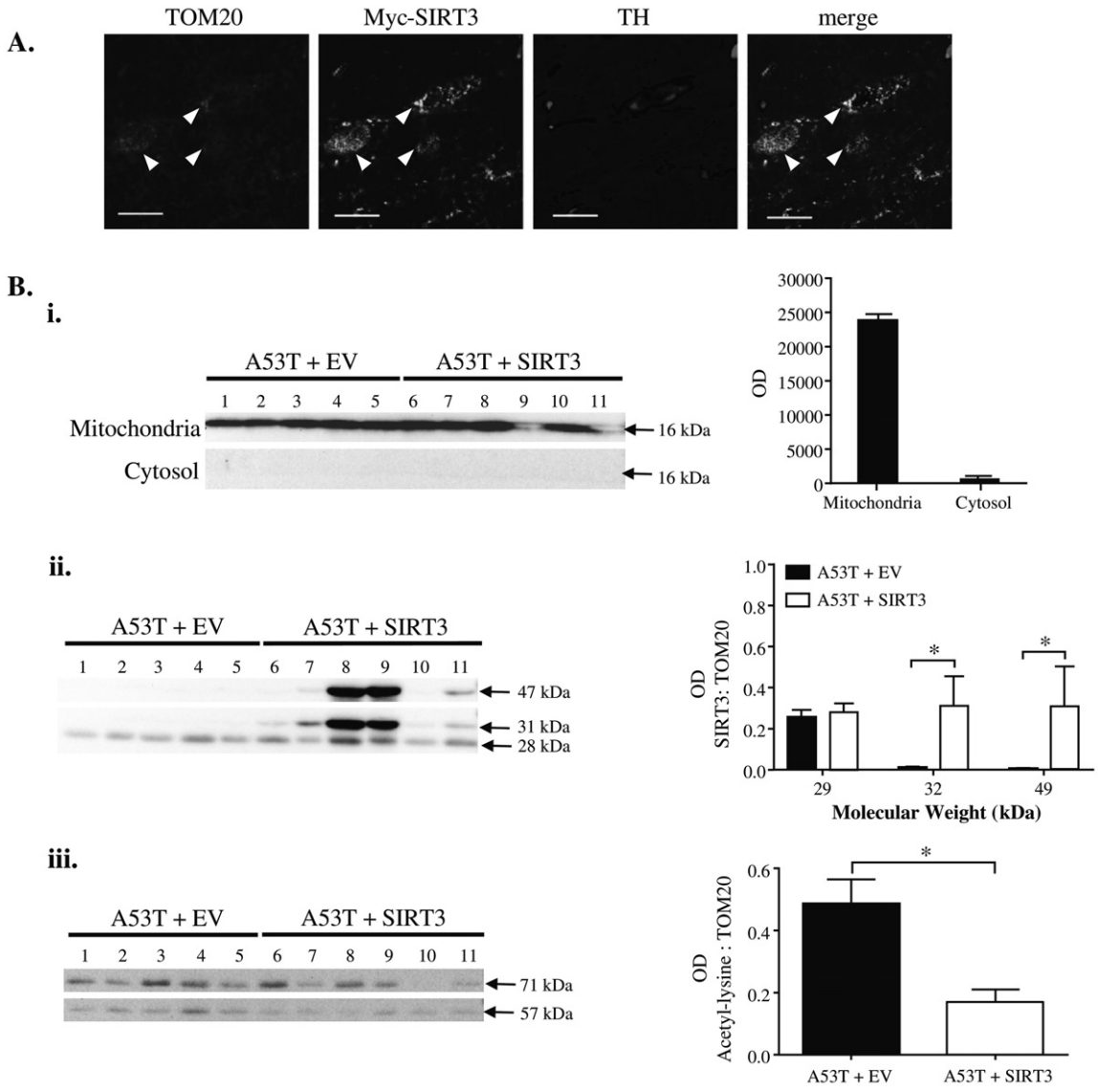

Fig. 6. SIRT3-myc expression in mitochondria of mutant (A53T) α-synuclein infected rats. On day 0, rats received intra-nigral injections of rAAV-A53T or EV. Eighteen days later, the same rats were administered rAAV SIRT3-myc or EV at the identical injection site. Six weeks following A53T injection, brains were processed to assess the subcellular localisation of SIRT3-myc and acetyl-lysine levels of mitochondria. A. Subcellular localisation of SIRT3-myc. Nigral sections of rat brain were exposed to antibodies against myc, TH and the mitochondrial protein, TOM20. Arrows indicate mitochondrial expression of SIRT3-myc. Scale bar = 20 μm. B. SIRT3 and acetyl-lysine levels in the mitochondria of the SN. Mitochondria were isolated from the SN of the AAV – injected hemisphere, then SDS-PAGE and Western Blotting performed. (i) Blots showing TOM20 (molecular weight 16 kDa) expression in mitochondrial and cytosolic fractions. Each lane represents one animal. The graph shows mean ± SEM OD of TOM20 in each fraction. (ii) Expression of endogenous SIRT3 and SIRT-myc in the mitochondria. The blots show the uncleaved and cleaved forms of SIRT3-myc (47 kDa and 31 kDa respectively) as well as the cleaved form of endogenous SIRT3 (28 kDa). The graph shows the mean ± SEM optical density of mitochondrial SIRT3 expression relative to TOM20 in parkinsonian (A53T + EV) and parkinsonian with SIRT3 (A53T + SIRT3-myc) rats ($n = 4–5$). (iii) Effect of SIRT3-myc on acetyl-lysine levels in the mitochondria. Representative blot and graph showing the mean ± SEM mitochondrial acetyl-lysine levels relative to TOM20 in A53T + EV and A53T + SIRT3-myc expressing rats ($n = 4–5$). For the graphs in panels 5B, lane 8 was removed from the analysis as the protein sample for this lane was taken from the same animal as lane 9. Also, lane 6 was removed from the study as it was a statistical outlier (median absolute deviation (Leys et al., 2013)) *$p < 0.05$ (Mann-Whitney *U* test).

This is the first demonstration that overexpression of SIRT3 is neuroprotective *in vivo* in a model of neurodegenerative disease, although other studies have shown that induction of SIRT3 is neuroprotective in cell models of Huntington's disease and ischemia, as well as in neuronal models of oxidative stress (Dai et al., 2017; Fu et al., 2012; Weir et al., 2012; Shulyakova et al., 2014; Song et al., 2013). Furthermore, in parkinsonism, absence of SIRT3 renders neurons more susceptible to cell death induced by the mitochondrial neurotoxin, MPTP *in* vivo (Liu et al., 2015). Also, in dopaminergic-cultured cells from DJ-1 knockout mice, lack of SIRT3 leaves neurons more sensitive to cell death, through the inactivation of the MnSOD pathway (Shi et al., 2017). However, despite the indirect evidence to suggest that ectopic introduction of SIRT3 has beneficial effects, some studies have shown the opposite, in that deletion of SIRT3 is neuroprotective (Novgorodov et al., 2016). In this later study, Nogorodov and colleagues compared a model of ischemia/reperfusion injury in SIRT3 knockout mice to wild-type mice, and showed that in ischemia, SIRT3 deacetylates the ceramide synthase, which is toxic to neurons (Novgorodov et al., 2016). Given this contradictory evidence that lack of SIRT3 is neuroprotective, combined with the absence of *in vivo* evidence for the neuroprotective effect of SIRT3, it was important to test the effect of ectopically introduced SIRT3, in a valid animal model of neurodegenerative disease. Our *in vivo* studies show that SIRT3 is protective when given prior to induction of parkinsonism, when neurons are healthy. Furthermore, our studies also show that, even if given at a time when cells are already undergoing cell stress, SIRT3 reverses cellular abnormalities to correct behavioural abnormalities, and prevents neurodegeneration. Given that patients with PD have lost approximately 50% of the dopaminergic nigro-striatal pathway

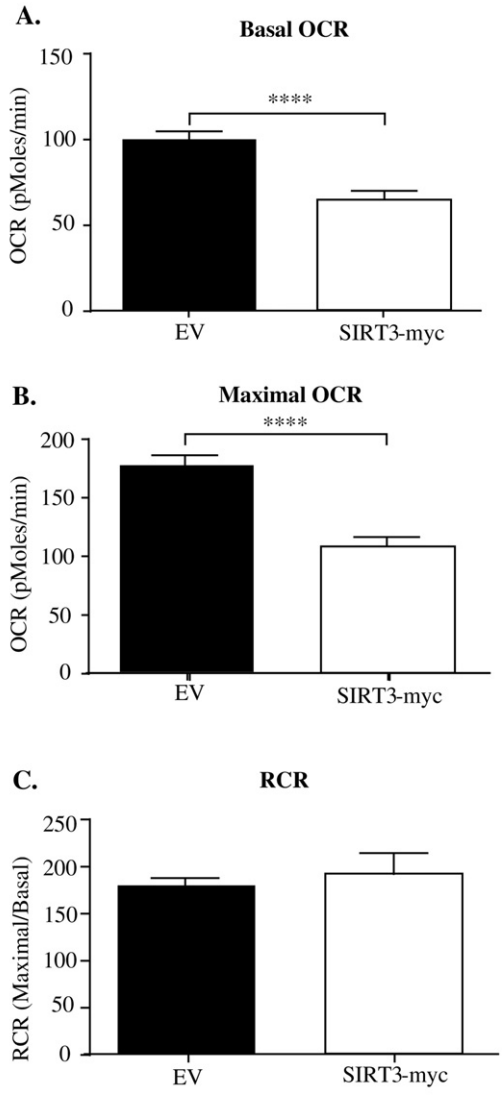

Fig. 7. Effect of SIRT3-myc on mitochondrial respiration in primary cultured neurons. Oxygen consumption rate (OCR) in mouse primary cultured dopaminergic neurons. (A) Basal respiration, (B) maximal respiration, (C) relative consumption rate (RCR). Values represented as mean ± SEM, $n = 10–30$ wells from at least 3 different cultures ****$p < 0.0001$ (Student two-tailed t-test).

when diagnosed, our findings suggest that SIRT3 may be able to not only protect the remaining population of nigro-striatal neurons, but also rescue the population of cells that are likely undergoing stress. Thus, SIRT3 has the potential to halt the progression of PD, preventing patients from reaching the more disabling, advanced stages of the disease.

Our studies show that in A53T rats, SIRT3-myc was solely expressed in the mitochondria, where it served as a protein deacetylase. We found no correlation between SIRT3-myc expression and percentage forelimb asymmetry, or protein acetylation levels. This may be due to the low sample size ($n = 4$) in our study on isolated mitochondria. An alternative explanation is that SIRT3-myc transduction is sufficiently high to cause an effect in all the animals following injection of this vector.

A recent study demonstrated that in the SNc, dopaminergic neurons have elevated mitochondrial bioenergetics demands compared to dopaminergic neurons in the ventral tegmental area and olfactory bulb, which makes them particularly vulnerable to oxidative stress (Pacelli et al., 2015). Thus, we determined how SIRT3-myc impacted mitochondrial function in primary dopaminergic neuronal cultures. Overexpression of SIRT3-myc decreased both basal and maximal OCR, which was associated with a small increase in the RCR, indicating that SIRT3 is able to give neurons a larger reserve of energy in order to meet changing demands, which would increase their resilience to stress. Our findings are in accordance with Pacelli and colleagues who showed that reducing the basal bioenergetics demands of nigral dopaminergic neurons by reducing s the development of their axonal arborisation leads to increased cell survival (Pacelli et al., 2015).

We further explored the effect of SIRT3 in mitochondria of human catecholaminergic neuroblastoma cells (SH-SY5Y) exposed to toxins which mimic several mechanisms linked with cell death processes involved in PD (Yong-Kee et al., 2012a; Yong-Kee et al., 2011; Yong-Kee et al., 2012b). Whilst these toxins are not directly linked to mutant synuclein-induced toxic mechanisms, they do cause mitochondrial dysfunction early in the cell death process (Yong-Kee et al., 2012a; Yong-Kee et al., 2011; Yong-Kee et al., 2012b), and so SIRT3 may protect mitochondria through similar mechanisms in neuroblastoma cells. Whilst cell models have many limitations, one being that they are far less representative of neurodegenerative disease in patients, these studies would be difficult to perform *in vivo*. SIRT3 prevented toxin – induced cell death, ROS production, and loss of ATP. These effects could be through the direct or indirect modulation of deacetylates SOD2 and catalase (Tseng et al., 2013; Sundaresan et al., 2009; Cheng et al., 2016; Kops et al., 2002) or isocitrate dehydrogenase 2 (Yu et al., 2012), all of which are SIRT3 substrates, to generate NADPH, which is a critical component of the mitochondrial antioxidant pathway (Yu et al., 2012). SIRT3-mediated inhibition of the mitochondrial permeability transition pore (mPTP) could also contribute to its neuroprotective effect, as mitochondrial calcium overload would be prevented, thus inhibiting induction of apoptosis (Dai et al., 2014; Hafner et al., 2010; Wu et al., 2013). Interestingly, we found that overexpression of SIRT3 caused a significant reduction in ATP levels compared to myc-expressing cells treated with vehicle. Possible mechanisms underlying the effect of SIRT3 on ATP include activation of uncoupling proteins (UCPs), or closure of the mPTP, as both are modulated directly and indirectly by SIRT3 (Hafner et al., 2010; Tseng et al., 2013; Cheng et al., 2016; Hafner et al., 2010; Correia et al., 2010; Ho et al., 2010). UCPs dissipate the proton motive force by actively leaking protons into the mitochondrial matrix, thereby decreasing Ψm. Through this mechanism, UCPs balance the generation of ATP whilst decreasing oxidative stress (Cornelius et al., 2013; Ramsden et al., 2012). Given that the deacetylase activity of SIRT3 is NAD^+-dependent, an alternative explanation for the decrease in ATP in SIRT3-expressing SH-SY5Y cells, and also for the decrease in OCD observed in primary cultured dopaminergic neurons cells could be reduced availability of NAD^+. If this were the case, rather than respiration being activated, as it would by UCP or mPTP activating proton dissipation at the inner mitochondrial membrane, basal respiration would be reduced, as we saw in primary dopaminergic neurons. The relationship between levels of NAD + and SIRT3-myc was not examined in the present study, so this possibility cannot be excluded. However, it is known that the mitochondria, particularly in neuronal cells have numerous mechanisms in place to prevent NAD depletion (Stein and Imai, 2012).

In conclusion, our studies show for the first time that overexpression of SIRT3 is neuroprotective and also prevents neurodegeneration by reversing neuronal stress in a rodent model of parkinsonism, which has previously been validated as appropriate for assessing potential disease-modifying agents. Our studies suggest that these effects are deacetylation-dependent, and are likely to be mediated by an increased efficiency of mitochondria, in a particularly energetically and homeostatically vulnerable population of dopaminergic neurons. It is likely that our observations are caused by the deacetylation of many SIRT3 substrates, which culminates to decrease metabolic rate through the stabilisation of respiration at the electron transport level, and reduction of oxidative stress. Similar energy-dissipating mechanisms have been established as cytoprotective in neurodegenerative diseases, including AD and ischemia (Cornelius et al., 2013; Mayanagi et al., 2007; Dirnagl and Meisel, 2008; Morris et al., 2011), and are also well

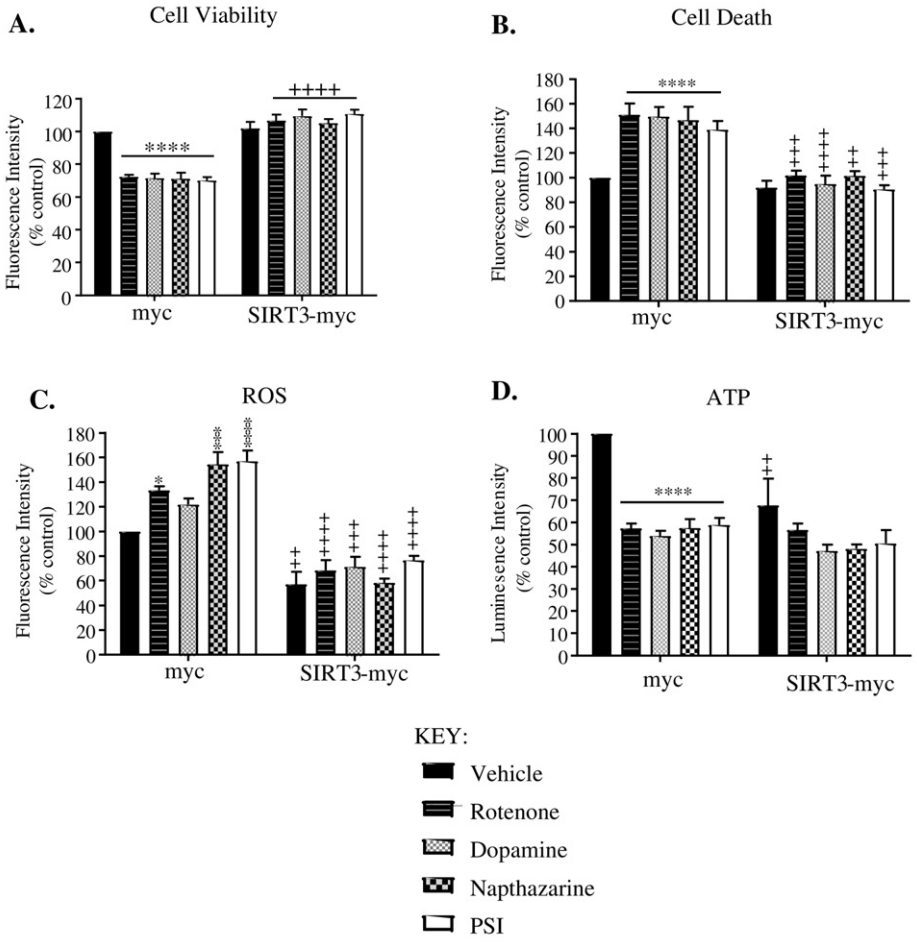

Fig. 8. Effect of SIRT3-myc on toxin exposure and mitochondrial function in SH-SY5Y cells. SH-SY5Y cells stably over-expressing SIRT3-myc or control (myc) were exposed to the following toxins: rotenone (30 nM), dopamine hydrochloride (65 μM), naphthazarin (300 nM), and PSI (30 nM). A. Cell viability measurements using Alamar blue. B. Cell death measurements using propidium iodide. C. Quantification of reactive oxygen species (ROS) using CM-H_2DCFA. **D.** ATP levels quantified using the Vialight kit. For all graphs, values are presented as mean ± SEM ($n = 4$). KEY: $^{*}p < 0.05$, $^{**}p < 0.01$, $^{***}p < 0.001$, $^{****}p < 0.0001$ - comparison between vehicle-treated and toxin-treated myc cells; $^{+}p < 0.05$, $^{++}p < 0.01$, $^{+++}p < 0.001$, $^{++++}p < 0.0001$ - comparison between myc and SIRT3-myc cells, same treatment group (ANOVA with Tukey *post-hoc*).

known therapies for obesity, where caloric restriction (CR), or therapies that mimic CR protect cells from stress through similar mechanisms (Weindruch et al., 1988; Liu et al., 2008; Guarente and Picard, 2005). Further supporting this explanation, SIRT3 activity is elevated following CR, which has been linked with the cytoprotective and longevity enhancing effects of CR (Dai et al., 2014; Wu et al., 2013; Morris et al., 2011; Guarente and Picard, 2005; Howitz et al., 2003).

Activation of SIRT3 is an excellent candidate for a disease-modifying therapeutic strategy in PD, as well as other neurodegenerative diseases which impact mitochondrial function, including AD, Huntington's disease and glaucoma. Furthermore, the serotype of AAV we used for overexpression of SIRT3, AAV1, has already been used in clinical trials, thus it is not unrealistic to suggest that targeted AAV-induced overexpression of SIRT3 in patients with PD could be used as a therapy (Greenberg et al., 2016; Mendell et al., 2015). Current studies are underway to further assess the value of SIRT3-myc AAV1 as a therapeutic agent in PD and other neurodegenerative diseases.

Supplementary data to this article can be found online at http://dx.doi.org/10.1016/j.nbd.2017.06.009.

Acknowledgements

We would like to thank Dr. Eric Verdin (UCSF, USA) for kindly supplying the deacetylase-deficient SIRT3^{H248Y}. We would also like to thank Dr. Philippe Monnier (Krembil Research Institute, Canada) for reviewing the manuscript prior to submission. Work in the Nash lab was financially supported by the Michael J. Fox Foundation, Parkinson Society Canada, NSERC and the University of Toronto. Work in the Trudeau lab was funded by the Brain Canada and Krembil foundations.

References

Ahn, B.H., Kim, H.S., Song, S., Lee, I.H., Liu, J., Vassilopoulos, A., Deng, C.X., Finkel, T., 2008. A role for the mitochondrial deacetylase Sirt3 in regulating energy homeostasis. Proc. Natl. Acad. Sci. U. S. A. 105 (38), 14447–14452.

Bao, J., Lu, Z., Joseph, J.J., Carabenciov, D., Dimond, C.C., Pang, L., Samsel, L., McCoy Jr., J.P., Leclerc, J., Nguyen, P., et al., 2010. Characterization of the murine SIRT3 mitochondrial localization sequence and comparison of mitochondrial enrichment and deacetylase activity of long and short SIRT3 isoforms. J. Cell Biochem. 110 (1), 238–247.

Bender, A., Krishnan, K.J., Morris, C.M., Taylor, G.A., Reeve, A.K., Perry, R.H., Jaros, E., Hersheson, J.S., Betts, J., Klopstock, T., et al., 2006. High levels of mitochondrial DNA deletions in substantia nigra neurons in aging and Parkinson disease. Nat. Genet. 38 (5), 515–517.

Burnett, C., Valentini, S., Cabreiro, F., Goss, M., Somogyvari, M., Piper, M.D., Hoddinott, M., Sutphin, G.L., Leko, V., McElwee, J.J., et al., 2011. Absence of effects of Sir2 overexpression on lifespan in *C. elegans* and drosophila. Nature 477 (7365), 482–485.

Chan, C.S., Gertler, T.S., Surmeier, D.J., 2010. A molecular basis for the increased vulnerability of substantia nigra dopamine neurons in aging and Parkinson's disease. Mov. Disord. 25 (Suppl. 1), S63–S70.

Cheng, A., Yang, Y., Zhou, Y., Maharana, C., Lu, D., Peng, W., Liu, Y., Wan, R., Marosi, K., Misiak, M., et al., 2016. Mitochondrial SIRT3 mediates adaptive responses of neurons to exercise and metabolic and excitatory challenges. Cell Metab. 23 (1), 128–142.

Chinopoulos, C., Zhang, S.F., Thomas, B., Ten, V., Starkov, A.A., 2011. Isolation and functional assessment of mitochondria from small amounts of mouse brain tissue. Methods Mol. Biol. 793, 311–324.
Cornelius, C., Trovato Salinaro, A., Scuto, M., Fronte, V., Cambria, M.T., Pennisi, M., Bella, R., Milone, P., Graziano, A., Crupi, R., et al., 2013. Cellular stress response, sirtuins and UCP proteins in Alzheimer disease: role of vitagenes. Immun. Ageing 10 (1), 41.
Correia, S.C., Santos, R.X., Perry, G., Zhu, X., Moreira, P.I., Smith, M.A., 2010. Mitochondria: the missing link between preconditioning and neuroprotection. J. Alzheimers Dis. 2 (20 Suppl), S475–S485.
Dai, S.H., Chen, T., Wang, Y.H., Zhu, J., Luo, P., Rao, W., Yang, Y.F., Fei, Z., Jiang, X.F., 2014. Sirt3 protects cortical neurons against oxidative stress via regulating mitochondrial Ca2+ and mitochondrial biogenesis. Int. J. Mol. Sci. 15 (8), 14591–14609.
Dai, S.H., Chen, T., Li, X., Yue, K.Y., Luo, P., Yang, L.K., Zhu, J., Wang, Y.H., Fei, Z., Jiang, X.F., 2017. Sirt3 confers protection against neuronal ischemia by inducing autophagy: involvement of the AMPK-mTOR pathway. Free Radic. Biol. Med. 108, 345–353.
Dirnagl, U., Meisel, A., 2008. Endogenous neuroprotection: mitochondria as gateways to cerebral preconditioning? Neuropharmacology 55 (3), 334–344.
Exner, N., Lutz, A.K., Haass, C., Winklhofer, K.F., 2012. Mitochondrial dysfunction in Parkinson's disease: molecular mechanisms and pathophysiological consequences. EMBO J. 31 (14), 3038–3062.
Fasano, C., Thibault, D., Trudeau, L.E., 2008. Culture of postnatal mesencephalic dopamine neurons on an astrocyte monolayer. Curr. Protoc. Neurosci. 44, 3.21.1–3.21.19 (Unit 3 21). (Chapter 3).
Fu, J., Jin, J., Cichewicz, R.H., Hageman, S.A., Ellis, T.K., Xiang, L., Peng, Q., Jiang, M., Arbez, N., Hotaling, K., et al., 2012. Trans-(−)-epsilon-viniferin increases mitochondrial sirtuin 3 (SIRT3), activates AMP-activated protein kinase (AMPK), and protects cells in models of Huntington disease. J. Biol. Chem. 287 (29), 24460–24472.
Greenberg, B., Butler, J., Felker, G.M., Ponikowski, P., Voors, A.A., Desai, A.S., Barnard, D., Bouchard, A., Jaski, B., Lyon, A.R., et al., 2016. Calcium upregulation by percutaneous administration of gene therapy in patients with cardiac disease (CUPID 2): a randomised, multinational, double-blind, placebo-controlled, phase 2b trial. Lancet 387 (10024), 1178–1186.
Guarente, L., Picard, F., 2005. Calorie restriction—the SIR2 connection. Cell 120 (4), 473–482.
Hafner, A.V., Dai, J., Gomes, A.P., Xiao, C.Y., Palmeira, C.M., Rosenzweig, A., Sinclair, D.A., 2010. Regulation of the mPTP by SIRT3-mediated deacetylation of CypD at lysine 166 suppresses age-related cardiac hypertrophy. Aging 2 (12), 914–923.
Hebert, A.S., Dittenhafer-Reed, K.E., Yu, W., Bailey, D.J., Selen, E.S., Boersma, M.D., Carson, J.J., Tonelli, M., Balloon, A.J., Higbee, A.J., et al., 2013. Calorie restriction and SIRT3 trigger global reprogramming of the mitochondrial protein acetylome. Mol. Cell 49 (1), 186–199.
Herskovits, A.Z., Guarente, L., 2013. Sirtuin deacetylases in neurodegenerative diseases of aging. Cell Res. 23 (6), 746–758.
Herskovits, A.Z., Guarente, L., 2014. SIRT1 in neurodevelopment and brain senescence. Neuron 81 (3), 471–483.
Ho, J.W., Ho, P.W., Zhang, W.Y., Liu, H.F., Kwok, K.H., Yiu, D.C., Chan, K.H., Kung, M.H., Ramsden, D.B., Ho, S.L., 2010. Transcriptional regulation of UCP4 by NF-kappaB and its role in mediating protection against MPP+ toxicity. Free Radic. Biol. Med. 49 (2), 192–204.
Howitz, K.T., Bitterman, K.J., Cohen, H.Y., Lamming, D.W., Lavu, S., Wood, J.G., Zipkin, R.E., Chung, P., Kisielewski, A., Zhang, L.L., et al., 2003. Small molecule activators of sirtuins extend *Saccharomyces cerevisiae* lifespan. Nature 425 (6954), 191–196.
Kim, H.S., Patel, K., Muldoon-Jacobs, K., Bisht, K.S., Aykin-Burns, N., Pennington, J.D., van der Meer, R., Nguyen, P., Savage, J., Owens, K.M., et al., 2010. SIRT3 is a mitochondria-localized tumor suppressor required for maintenance of mitochondrial integrity and metabolism during stress. Cancer Cell 17 (1), 41–52.
Koprich, J.B., Johnston, T.H., Reyes, M.G., Sun, X., Brotchie, J.M., 2010. Expression of human A53T alpha-synuclein in the rat substantia nigra using a novel AAV1/2 vector produces a rapidly evolving pathology with protein aggregation, dystrophic neurite architecture and nigrostriatal degeneration with potential to model the pathology of Parkinson's disease. Mol. Neurodegener. 5, 43.
Koprich, J.B., Johnston, T.H., Huot, P., Reyes, M.G., Espinosa, M., Brotchie, J.M., 2011. Progressive neurodegeneration or endogenous compensation in an animal model of Parkinson's disease produced by decreasing doses of alpha-synuclein. PLoS One 6 (3), e17698.
Kops, G.J., Dansen, T.B., Polderman, P.E., Saarloos, I., Wirtz, K.W., Coffer, P.J., Huang, T.T., Bos, J.L., Medema, R.H., Burgering, B.M., 2002. Forkhead transcription factor FOXO3a protects quiescent cells from oxidative stress. Nature 419 (6904), 316–321.
Kyrylenko, S., Baniahmad, A., 2010. Sirtuin family: a link to metabolic signaling and senescence. Curr. Med. Chem. 17 (26), 2921–2932.
Leys, C., Klein, O., Bernard, P., Licata, L., 2013. Detecting outliers: do not use standard deviation around the mean, use absolute deviation around the median. J. Exp. Soc. Psychol. 49 (4), 764–766.
Liu, D., Pitta, M., Mattson, M.P., 2008. Preventing NAD(+) depletion protects neurons against excitotoxicity: bioenergetic effects of mild mitochondrial uncoupling and caloric restriction. Ann. N. Y. Acad. Sci. 1147, 275–282.
Liu, L., Peritore, C., Ginsberg, J., Kayhan, M., Donmez, G., 2015. SIRT3 attenuates MPTP-induced nigrostriatal degeneration via enhancing mitochondrial antioxidant capacity. Neurochem. Res. 40, 600–608.
Lombard, D.B., Alt, F.W., Cheng, H.L., Bunkenborg, J., Streeper, R.S., Mostoslavsky, R., Kim, J., Yancopoulos, G., Valenzuela, D., Murphy, A., et al., 2007. Mammalian Sir2 homolog SIRT3 regulates global mitochondrial lysine acetylation. Mol. Cell. Biol. 27 (24), 8807–8814.
Lucking, C.B., Durr, A., Bonifati, V., Vaughan, J., De Michele, G., Gasser, T., Harhangi, B.S., Meco, G., Denefle, P., Wood, N.W., et al., 2000. Association between early-onset Parkinson's disease and mutations in the parkin gene. N. Engl. J. Med. 342 (21), 1560–1567.
Matsuda, N., Sato, S., Shiba, K., Okatsu, K., Saisho, K., Gautier, C.A., Sou, Y.S., Saiki, S., Kawajiri, S., Sato, F., et al., 2010. PINK1 stabilized by mitochondrial depolarization recruits parkin to damaged mitochondria and activates latent parkin for mitophagy. J. Cell Biol. 189 (2), 211–221.
Mayanagi, K., Gaspar, T., Katakam, P.V., Kis, B., Busija, D.W., 2007. The mitochondrial K(ATP) channel opener BMS-191095 reduces neuronal damage after transient focal cerebral ischemia in rats. J. Cereb. Blood Flow Metab. 27 (2), 348–355.
McFarland, N.R., Lee, J.S., Hyman, B.T., McLean, P.J., 2009. Comparison of transduction efficiency of recombinant AAV serotypes 1, 2, 5, and 8 in the rat nigrostriatal system. J. Neurochem. 109 (3), 838–845.
Mendell, J.R., Sahenk, Z., Malik, V., Gomez, A.M., Flanigan, K.M., Lowes, L.P., Alfano, L.N., Berry, K., Meadows, E., Lewis, S., et al., 2015. A phase 1/2a follistatin gene therapy trial for becker muscular dystrophy. Mol. Ther. 23 (1), 192–201.
Morris, K.C., Lin, H.W., Thompson, J.W., Perez-Pinzon, M.A., 2011. Pathways for ischemic cytoprotection: role of sirtuins in caloric restriction, resveratrol, and ischemic preconditioning. J. Cereb. Blood Flow Metab. 31 (4), 1003–1019.
Nogueiras, R., Habegger, K.M., Chaudhary, N., Finan, B., Banks, A.S., Dietrich, M.O., Horvath, T.L., Sinclair, D.A., Pfluger, P.T., Tschop, M.H., 2012. Sirtuin 1 and sirtuin 3: physiological modulators of metabolism. Physiol. Rev. 92 (3), 1479–1514.
Novgorodov, S.A., Riley, C.L., Keffler, J.A., Yu, J., Kindy, M.S., Macklin, W.B., Lombard, D.B., Gudz, T.I., 2016. SIRT3 deacetylates ceramide synthases: implications for mitochondrial dysfunction and brain injury. J. Biol. Chem. 291 (4), 1957–1973.
Pacelli, C., Giguere, N., Bourque, M.J., Levesque, M., Slack, R.S., Trudeau, L.E., 2015. Elevated mitochondrial bioenergetics and axonal arborization size are key contributors to the vulnerability of dopamine neurons. Curr. Biol. 25 (18), 2349–2360.
Paxinos, G., Watson, C., 1998. The Rat Brain in Stereotaxic Coordinates. Academic Press.
Ramsden, D.B., Ho, P.W., Ho, J.W., Liu, H.F., So, D.H., Tse, H.M., Chan, K.H., Ho, S.L., 2012. Human neuronal uncoupling proteins 4 and 5 (UCP4 and UCP5): structural properties, regulation, and physiological role in protection against oxidative stress and mitochondrial dysfunction. Brain Behav. 2 (4), 468–478.
Reeve, A.K., Krishnan, K.J., Turnbull, D., 2008. Mitochondrial DNA mutations in disease, aging, and neurodegeneration. Ann. N. Y. Acad. Sci. 1147, 21–29.
Schapira, A.H., Mann, V.M., Cooper, J.M., Krige, D., Jenner, P.J., Marsden, C.D., 1992. Mitochondrial function in Parkinson's disease. The Royal Kings and Queens Parkinson's Disease Research Group. Ann. Neurol. (32 Suppl), S116–S124.
Scher, M.B., Vaquero, A., Reinberg, D., 2007. SirT3 is a nuclear NAD+-dependent histone deacetylase that translocates to the mitochondria upon cellular stress. Genes Dev. 21 (8), 920–928.
Shi, T., Wang, F., Stieren, E., Tong, Q., 2005. SIRT3, a mitochondrial sirtuin deacetylase, regulates mitochondrial function and thermogenesis in brown adipocytes. J. Biol. Chem. 280 (14), 13560–13567.
Shi, H., Deng, H.X., Gius, D., Schumacker, P.T., James Surmeier, D., Ma, Y.C., 2017. Sirt3 protects dopaminergic neurons from mitochondrial oxidative stress. Hum. Mol. Genet. 26 (10), 1915–1926.
Shimazu, T., Hirschey, M.D., Hua, L., Dittenhafer-Reed, K.E., Schwer, B., Lombard, D.B., Li, Y., Bunkenborg, J., Alt, F.W., Denu, J.M., et al., 2010. SIRT3 deacetylates mitochondrial 3-hydroxy-3-methylglutaryl CoA synthase 2 and regulates ketone body production. Cell Metab. 12 (6), 654–661.
Shulyakova, N., Sidorova-Darmos, E., Fong, J., Zhang, G., Mills, L.R., Eubanks, J.H., 2014. Over-expression of the Sirt3 sirtuin protects neuronally differentiated PC12 Cells from degeneration induced by oxidative stress and trophic withdrawal. Brain Res. 1587, 40–53.
Sidorova-Darmos, E., Wither, R.G., Shulyakova, N., Fisher, C., Ratnam, M., Aarts, M., Lilge, L., Monnier, P.P., Eubanks, J.H., 2014. Differential expression of sirtuin family members in the developing, adult, and aged rat brain. Front. Aging Neurosci. 6, 333.
Someya, S., Yu, W., Hallows, W.C., Xu, J., Vann, J.M., Leeuwenburgh, C., Tanokura, M., Denu, J.M., Prolla, T.A., 2010. Sirt3 mediates reduction of oxidative damage and prevention of age-related hearing loss under caloric restriction. Cell 143 (5), 802–812.
Song, W., Song, Y., Kincaid, B., Bossy, B., Bossy-Wetzel, E., 2013. Mutant SOD1G93A triggers mitochondrial fragmentation in spinal cord motor neurons: neuroprotection by SIRT3 and PGC-1 alpha. Neurobiol. Dis. 51, 72–81.
Stein, L.R., Imai, S., 2012. The dynamic regulation of NAD metabolism in mitochondria. Trends Endocrinol. Metab. 23 (9), 420–428.
Sundaresan, N.R., Gupta, M., Kim, G., Rajamohan, S.B., Isbatan, A., Gupta, M.P., 2009. Sirt3 blocks the cardiac hypertrophic response by augmenting Foxo3a-dependent antioxidant defense mechanisms in mice. J. Clin. Invest. 119 (9), 2758–2771.
Surmeier, D.J., 2007. Calcium, ageing, and neuronal vulnerability in Parkinson's disease. Lancet Neurol. 6 (10), 933–938.
Surmeier, D.J., Guzman, J.N., Sanchez-Padilla, J., 2010. Calcium, cellular aging, and selective neuronal vulnerability in Parkinson's disease. Cell Calcium 47 (2), 175–182.
Tseng, A.H., Shieh, S.S., Wang, D.L., 2013. SIRT3 deacetylates FOXO3 to protect mitochondria against oxidative damage. Free Radic. Biol. Med. 63, 222–234.
Valente, E.M., Abou-Sleiman, P.M., Caputo, V., Muqit, M.M., Harvey, K., Gispert, S., Ali, Z., Del Turco, D., Bentivoglio, A.R., Healy, D.G., et al., 2004. Hereditary early-onset Parkinson's disease caused by mutations in PINK1. Science 304 (5674), 1158–1160.
Weindruch, R., Naylor, P.H., Goldstein, A.L., Walford, R.L., 1988. Influences of aging and dietary restriction on serum thymosin alpha 1 levels in mice. J. Gerontol. 43 (2), B40–B42.
Weir, H.J., Murray, T.K., Kehoe, P.G., Love, S., Verdin, E.M., O'Neill, M.J., Lane, J.D., Balthasar, N., 2012. CNS SIRT3 expression is altered by reactive oxygen species and in Alzheimer's disease. PLoS One 7 (11), e48225.
Whishaw, I.Q., Kolb, B., 2005. The Behavior of the Laboratory Rat: A Handbook With Tests. Oxford University Press, Oxford, New York.

Wu, J.J., Cui, Y., Yang, Y.S., Jung, S.C., Hyun, J.W., Maeng, Y.H., Park, D.B., Lee, S.R., Kim, S.J., Eun, S.Y., 2013. Mild mitochondrial depolarization is involved in a neuroprotective mechanism of citrus sunki peel extract. Phytother. Res. 27 (4), 564–571.

Yong-Kee, C.J., Salomonczyk, D., Nash, J.E., 2011. Development and validation of a screening assay for the evaluation of putative neuroprotective agents in the treatment of Parkinson's disease. Neurotox. Res. 19 (4), 519–526.

Yong-Kee, C.J., Sidorova, E., Hanif, A., Perera, G., Nash, J.E., 2012a. Mitochondrial dysfunction precedes other sub-cellular abnormalities in an in vitro model linked with cell death in Parkinson's disease. Neurotox. Res. 21 (2), 185–194.

Yong-Kee, C.J., Warre, R., Monnier, P.P., Lozano, A.M., Nash, J.E., 2012b. Evidence for synergism between cell death mechanisms in a cellular model of neurodegeneration in Parkinson's disease. Neurotox. Res. 22 (4), 355–364.

Yu, W., Dittenhafer-Reed, K.E., Denu, J.M., 2012. SIRT3 protein deacetylates isocitrate dehydrogenase 2 (IDH2) and regulates mitochondrial redox status. J. Biol. Chem. 287 (17), 14078–14086.

Zhang, B.R., Hu, Z.X., Yin, X.Z., Cai, M., Zhao, G.H., Liu, Z.R., Luo, W., 2010. Mutation analysis of parkin and PINK1 genes in early-onset Parkinson's disease in China. Neurosci. Lett. 477 (1), 19–22.